Experimental control of a chaotic pendulum with unknown dynamics using delay coordinates

Robert Jan de Korte, Jaap C. Schouten, and Cor M. van den Bleek
Department of Chemical Process Technology, Delft University of Technology, Julianalaan 136, 2628 BL Delft, The Netherlands
(Received 13 June 1995)

Unstable periodic orbits (UPOs) of an experimental chaotic pendulum were stabilized using a semicontinuous control method (SCC), applying control actions several times per cycle. One advantage of this method, compared to a one-map-based control method such as the Ott-Grebogi-Yorke method [Phys. Rev. Lett. **64**, 1196 (1990)], is the applicability to systems with relatively large unstable eigenvalues and/or high noise levels. Compared to a continuous type of feedback control as was proposed by Pyragas [Phys. Lett. A **170**, 421 (1992)], the advantage is that the controller settings can be measured from experimental data. Because the control method uses delay coordinates, only one variable has to be measured. This paper describes an SCC method using delay coordinates, the extraction of UPOs from time series, how the effect of the control parameter can be measured, the effect on the control in case of an error in the estimate of the UPO, and how this error can be reduced to obtain more stable control.

PACS number(s): 05.45.+b

I. INTRODUCTION

The extreme sensitivity to small perturbations is a well-known characteristic of chaotic systems. Since 1990, in literature, much attention has been paid to the idea of exploiting this sensitivity as an advantage in controlling the dynamics of chaotic systems. As a consequence, only small control actions would be necessary to drive the system into one of its required states. In the important paper on this topic, Ott, Grebogi, and Yorke (OGY) [1] proposed such a method. In the attractor, many so-called unstable periodic orbits (UPOs) are located. If the system were to be located *exactly* on a UPO, it would remain there forever. However, because of the chaotic nature, a small deviation will grow exponentially in time so that the system eventually leaves its periodic orbit. The OGY control method is essentially based on feedback control that stabilizes the system on a UPO. Because each UPO has its own system performance, one would like to stabilize only that UPO with a system performance that is better than that of the uncontrolled system. The advantage is that only very small control actions are required for the stabilization. This may be very attractive, especially from a practical point of view: generally, small control actions are physically easy to make and do not demand much energy. So this method would allow improvement to the performance of an existing system, without making physical modifications. The OGY control method is of a discrete type; a control action is made only once per periodic orbit.

Application of the discrete OGY control method to simple experimental systems has resulted in some successes; see the review article by Shinbrot *et al.* [2] for some examples and Starret and Tagg [3] for a type of chaotic pendulum. For chaotic systems with very unstable periodic orbits (viz., large Lyapunov exponents) or with a high level of noise, a continuous type of control would be more appropriate. This means that if there is a deviation from the UPO, control action should be taken immediately so that the deviation has no opportunity to grow. A continuous control method to stabilize UPOs was proposed by Pyragas [4], which can work even if the UPO is unknown; see also Kittel, Parisi, and Pyragas [5]. For instance, laser systems were successfully stabilized by this method [6]. Somewhere between the discrete control method and the continuous control method, one can think of a "semicontinuous control" method (SCC), which applies control actions not continuously but several times a period. In literature two of these control types are reported, the "local control method" by Hübinger *et al.* [7] and the "minimal expected deviation" (MED) method by Reyl *et al.* [8]. Advantages of this type of control compared to continuous control are that (i) the feedback control parameters can be different for different places on an UPO and that (ii) it is possible to "measure" the feedback control parameters, which is difficult for a continuous controller.

In this paper, it is discussed how a chaotic driven damped pendulum with large unstable eigenvalues (about ten) was successfully controlled using a SCC method. This work can be seen as an extension to the control of a different pendulum by Hübinger *et al.* [7]. The major difference is the use of delay coordinates, with the advantage that now the method is also applicable to systems in which only one system variable can be measured. In this case, the angular velocity cannot be measured accurately. Because the mathematical description of the pendulum was unknown, all feedback constants had to be extracted from experimental data; for this a different approach was used. Section II describes the theory of the extended SCC method and how experimental data was gathered to finally control the pendulum's dynamics, and attention is paid to the behavior of the controlled system.

II. THEORY

The SCC method is based on measuring transition maps of the system. The transition maps relate the sys-

tem state in one surface of section to the system state in the next section. A Poincaré map is a special case of such a transition map, where the mapping is one complete cycle ahead. As the pendulum has three degrees of freedom, its transition maps have two; see Fig. 1. For convenience, the method will be explained for two-dimensional maps, although it could be extended to systems with a higher dimension. Consider a two-dimensional surface of section on which the system state can be represented by a delay vector $\vec{Z}$ at time $t=t^n$ (superscript n is the discrete time index) containing two elements of the continuous time variable $\theta(t)$. There is a delay time T_D between the first and second element,

$$\vec{Z}^n=\begin{bmatrix}\theta(t=t^n)\\ \theta(t=t^n-T_D)\end{bmatrix}. \tag{1}$$

If the system was not perturbed, there would be a map $\vec{Z}^{n+1}=\vec{F}(\vec{Z}^n)$, from one intersection point $\vec{Z}^n$ on the control section to the next $\vec{Z}^{n+1}$, with $\vec{F}$ a fixed but unknown function. Suppose there is an externally adjustable control parameter p that can be varied around a value $\bar{p}$ such that $|p-\bar{p}|=|\delta p|<\delta p_{\max}$ in order to influence the system. If $\vec{Z}$ would contain the real system state (so not represented by delay coordinates), then the map would be of the form $\vec{Z}^{n+1}=\vec{F}(\vec{Z}^n,\delta p^n)$. In the case of delay coordinates, it was shown by Dressler and Nitsche [9] that the map becomes of the extended form

$$\vec{Z}^{n+1}=\vec{F}(\vec{Z}^n,\delta p^n,\delta p^{n-1},\ldots,\delta p^{n-r}). \tag{2}$$

The reconstructed system state $\vec{Z}^{n+1}$ not only depends on δp^n, but also on all previous values of δp, viz., $\delta p^{n-1},\ldots,\delta p^{n-r}$, that influence the system during the time interval $t^n-T_D\le t\le t^n$ (with r as the largest possible integer such that δp^{n-r} lies still in this interval). In practice, one likes to choose the total time delay T_D shorter than the time between the piercings of the sections $\vec{Z}^n$ and $\vec{Z}^{n+1}$. In that case only *one* previous control action has to be taken into account,

$$\vec{Z}^{n+1}=\vec{F}(\vec{Z}^n,\delta p^n,\delta p^{n-1}). \tag{3}$$

Stabilization of an UPO corresponds to stabilizing the so-called fixed points $\vec{Z}_*$ these points are the intersection points of the UPO with the control sections. Now suppose that a number of N control sections per cycle is used for stabilizing an UPO; in that case, there are N fixed points $\vec{Z}_*^1,\ldots,Z_*^N$, the discrete time n can be counted as n modulo N. Linearization of Eq. (3) around the fixed point and using deviation variables $\delta\vec{Z}^n=\vec{Z}^n-\vec{Z}_*^n$ results in

$$\delta\vec{Z}^{n+1}=\mathbf{A}^n\delta\vec{Z}^n+\vec{B}_0^n\delta p^n+\vec{B}_1^n\delta p^{n-1}, \tag{4}$$

where $\mathbf{A}^n=\mathbf{D}_{\vec{Z}^n}\vec{F}(\vec{Z}^n,\delta p^n,\delta p^{n-1})$ is a 2×2 Jacobian matrix, and $\vec{B}_0^n=\mathbf{D}_{\delta p^n}\vec{F}(\vec{Z},\delta p^n,\delta p^{n-1})$ and $\vec{B}_1^n=\mathbf{D}_{\delta p^{n-1}}\vec{F}(\vec{Z},\delta p^n,\delta p^{n-1})$ are two-dimensional column vectors. These 3 times N partial derivatives are evaluated at the N unperturbed fixed points $(\vec{Z}_*^1,\ldots,\vec{Z}_*^N$ for $\delta p=0)$. Equation (4) predicts where the system will be on the next section. At time n, the prediction one step ahead consists of two parts: one part $(\mathbf{A}^n\delta\vec{Z}^n+\vec{B}_1^n\delta p^{n-1})$ is a result of history and cannot be changed anymore, the other part $(\vec{B}_0^n\delta p^n)$ can still be changed by controlling δp^n. Figure 2 shows the graphical representation; if at time n no perturbation is applied, the system will arrive at the point $\vec{Z}^{n+1}(\delta p^n=0)$. By controlling δp^n, the system can be directed to any location on the line through $\vec{Z}^{n+1}(\delta p^n=0)$ with direction $\vec{B}_0$. This is where one has to choose a control criterion. One could, for instance, choose δp^n such that the distance to the fixed point becomes minimal (minimal expected deviation method, [8]). However, this will not always result in a stable control because it is very possible that the point with the minimal expected deviation lies near the unstable manifold of the Poincaré map, so that the system's trajectory will tend to leave the UPO immediate-

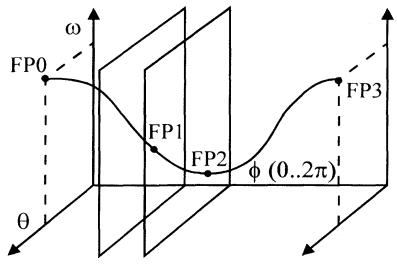

FIG. 1. The state space of the pendulum contains the angular velocity ω (rad/s), the angle θ (rad), and the phase of the driving torque ϕ between 0 and 2π. A point of intersection between an UPO and the surface of section is called a fixed point (FP 0, 1, 2, 3). The periodic orbit has the same angular velocity and angle at phase $\phi=0$ and $\phi=2\pi$ (FP0=FP3). For delay coordinates, the angular velocity is replaced by a previous value of the angle. Two surfaces of section are shown, and a transition map exists $\vec{Z}^2=\vec{F}(\vec{Z}^1)$, from a point on section 1 to a point on section 2.

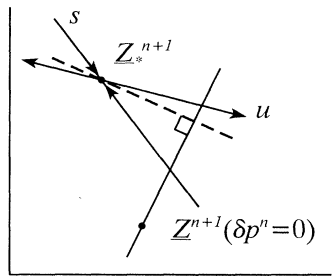

FIG. 2. Transition map of the system state $\vec{Z}^{n+1}$ near fixed point $\vec{Z}_*^{n+1}$; lines s and u indicate the stable and unstable manifolds, respectively. If the system is on a stable or unstable manifold, it is attracted or repulsed, respectively, in the direction of that manifold. If at time n no control action is made, the system will come in state $\vec{Z}^{n+1}(\delta p^n=0)$, and this point can be shifted in the direction determined by $\vec{B}_0^n$ by modifying δp^n. Minimizing the expected deviation (construction with perpendicular dashed line) may not lead to stability if the target point is too close to the unstable manifold.

ly after the deviation was minimal only at time $n+1$.

So it is necessary to consider the stabilizing and destabilizing directions near the fixed point. Hübinger *et al.* [7] used the singular value decomposition

$$\mathbf{A}^n=\mathbf{U}^n\mathbf{\Sigma}^n(\mathbf{V}^n)^T=[\vec{u}_1^{\,n}\ \ \vec{u}_2^{\,n}]\begin{bmatrix}\sigma_1^n & 0\\ 0 & \sigma_2^n\end{bmatrix}[\vec{v}_1^{\,n}\ \ \vec{v}_2^{\,n}]^T, \quad (5)$$

to calculate how a unit circle around the fixed point is transformed into an ellipsoid by the linear operation $\mathbf{A}^n\delta\vec{Z}^n$; see Fig. 3. A control formula could be derived by demanding that the projection on the maximum stretching direction reduces (with about 15%; see Hübinger *et al.* [10]) for each control section. This reduction in their case could only be 15% to avoid singularity in the control formula that resulted from the large number of maps used (64). We use a smaller number of control sections to make the measuring of the partial derivatives of Eq. (4) easier (see also next paragraph), so no singularity will occur and a different control formula can be derived in which no extra parameter, like the shrinking percentage, has to be chosen.

The two unit axes ($\vec{v}_1$ and $\vec{v}_2$) correspond to the long and short axis ($\sigma_1\vec{u}_1$ and $\sigma_2\vec{u}_2$) on the ellipsoid. Now the control target becomes to adjust δp^n such that on the map at time $n+1$ the direction $\vec{v}_2$ is obtained, resulting in a maximal shrinking on map $n+2$; see Fig. 3. So we demand $\delta\vec{Z}^{n+1}=l\vec{v}_2^{\,n+1}$, with l the length of the maximal shrinking direction ($\vec{v}_2$ has been normalized), or

$$\mathbf{A}^n\delta\vec{Z}^n+\vec{B}_0^n\delta p^n+\vec{B}_1^n\delta p^{n-1}=l\vec{v}_2^{\,n+1}. \quad (6)$$

For higher dimensional systems, one could demand that the projection on the maximal expanding direction becomes zero. Equation (6) can be written as two equations for δp^n and l (lowercase symbols indicate elements of vector or matrix):

$$\begin{bmatrix}b_{0,1}^n\delta p^n-lv_{2,1}^{n+1}\\ b_{0,2}^n\delta p^n-lv_{2,2}^{n+1}\end{bmatrix}=-\begin{bmatrix}a_{11}^n & a_{12}^n & b_{1,1}^n\\ a_{21}^n & a_{22}^n & b_{1,2}^n\end{bmatrix}\begin{bmatrix}\delta z_1^n\\ \delta z_2^n\\ \delta p^{n-1}\end{bmatrix}, \quad (7)$$

which gives

$$\delta p^n=\frac{-1}{b_{0,1}^n-Rb_{0,2}^n}(a_{11}^n-Ra_{21}^n\ \ a_{12}^n-Ra_{22}^n\ \ b_{1,1}^n-Rb_{1,2}^n)\times\begin{bmatrix}\delta z_1^n\\ \delta z_2^n\\ \delta p^{n-1}\end{bmatrix}, \quad (8)$$

with

$$R=\frac{v_{2,1}^{n+1}}{v_{2,2}^{n+1}}. \quad (9)$$

So what basically remains is a simple kind of proportional feedback control of the form $\delta p^n=\mathbf{K}^n[(\delta\vec{Z}^n)^T\delta p^{n-1}]^T$. This form looks very much the same as the original OGY control formula, except that it is extended with an extra term δp^{n-1} because of the use of delay coordinates, and that the constant feedback matrices $\mathbf{K}^n$ are computed in a different way. Therefore, this SCC method also requires an almost equally short computation time *per section.*

III. EXPERIMENTAL SETUP

The pendulum used (see Fig. 4) is a type EM-50 chaotic pendulum produced by the Daedalon Corporation (Salem, MA, USA). The pendulum arm itself is connected to an axis with an optical encoder wheel and a ring magnet attached to it. Four electromagnetic drive coils act as a motor that generates a torque acting on the ring magnet. So the system has three degrees of freedom: angle θ, angular velocity ω, and driving phase ϕ. The optical encoder wheel contains a large number of small slots

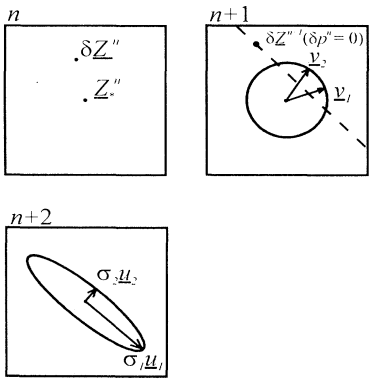

FIG. 3. Three successive maps of the system indicating the principle of the control formula. The dot at the center of the maps indicates its fixed point. At time n, the system can be steered to any point on the dashed line through $\delta\vec{Z}^{n+1}(\delta p^n=0)$ with direction $\vec{B}_0^n$. Now as a control criterion, the choice is made to steer to axis $\vec{v}_2$ that corresponds with the maximal shrinking axis $\sigma_2\vec{u}_2$ at the next transition map at time $n+2$.

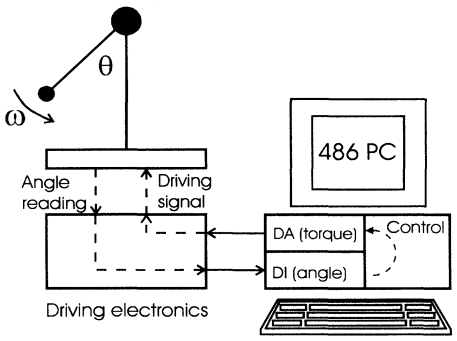

FIG. 4. Schematic setup of the pendulum. The pendulum arm can rotate around an axis. The angle of the pendulum θ is measured, from which the control algorithm can calculate the required control actions δp. These are added to a sinusoidal wave and form the total applied driving signal (torque).

that can optically be detected so that the angle of the pendulum can be measured with a resolution of 4000 positions ($=2\pi$ rad). An 80486-based computer with a digital-to-analog (DA) converter generates a sinusoidal voltage that is transformed to a sinusoidal torque by the pendulum's electronics and driving mechanism. The frequency of this voltage is $f=0.85$ Hz. If the pendulum is at rest (no torque acting on it), it does not hang straight downwards with gravity but an angle of about 10°. This is caused by the fact that the four electromagnetic coils repulse the pendulum for certain positions (up, down, left, right). This causes that determination of a model (description by a differential equation) for the pendulum together with its parameters, is quite a complex task. For controlling the pendulum however, no differential equation is needed because UPOs and controller constants can be extracted from time series.

IV. SEARCH FOR PERIODIC ORBITS

Because the pendulum is periodically forced, a simple stroboscopic Poincaré map can be constructed by sampling the angle at a constant value of the driving phase ϕ ($\phi=2\pi ft \bmod 2\pi$). Figure 5 shows an example of a Poincaré map with the angle at phase $\phi=2\pi$ plotted against that at phase $\phi=7/4\pi$. In order to locate fixed points for all points on this Poincaré map, it has to be checked whether the next point on the map is close to the previous one. The criterion for this was taken as $|\vec{Z}^{n+N}-\vec{Z}^{n}|<0.05\times 2\pi$. These pairs of close returning points (CRPs) indicate the *possible* presence of a fixed point nearby. Figure 6 shows these CRPs that are more or less grouped, each group belonging to a different fixed point. The task is now to calculate the *exact* position of a fixed point from these CRPs. It could be tried to (least square) fit these points to a linear relation, as mentioned

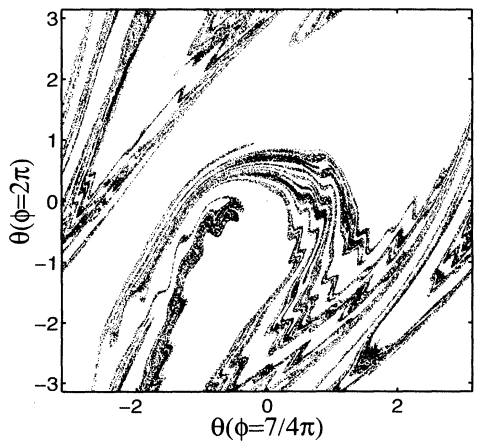

FIG. 5. Poincaré map with 45 000 points of the pendulum with the angle θ (rad) at phase $\phi=2\pi$ plotted against the delayed angle θ (rad) at phase $\phi=7/4\pi$.

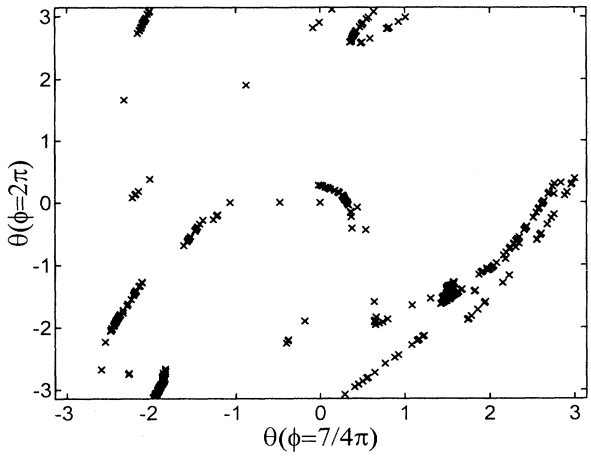

FIG. 6. Poincaré map showing CRPs. Every point on this figure has a successor at a distance smaller than $0.05\times 2\pi$ rad. The points are located in groups that belong to different fixed points. The groups are not spread uniformly, but the points are located along stabilizing directions.

by Shinbrot *et al.* [2]:

$$\vec{Z}^{n+N}=\mathbf{M}\vec{Z}^{n}+\vec{C}\ , \tag{10}$$

and, especially if noise is present, one would like to use many CRPs to fit $\mathbf{M}$ and $\vec{C}$. Then the location of the fixed point will be obtained by setting $\vec{Z}^{n+N}=\vec{Z}^{n}=\vec{Z}_{*}$, so that $\vec{Z}_{*}=(1-\mathbf{M})^{-1}\vec{C}$. This method was initially tried but the error of the fit proved to be much larger than the experimental error of the pendulum's angle reading (≈ 1 position out of 4000). This is caused by the severe nonlinear dynamics that makes linear model predictions that are one complete cycle ahead hardly possible. Obtaining a good fit becomes even more complicated when the points are not uniformly spread around a fixed point, but are directed along a stable direction, while their successors are directed along an unstable direction, which is what seems to be the case in Fig. 6. Perhaps if CRPs with much shorter distances than $0.05\times 2\pi$ rad are selected to fit Eq. (10), the linear model could still be used. The frequency at which these points occur on the map is very low, which means that a very long time series has to be measured to get enough CRPs. Even for this pendulum with its low-dimensional attractor, this could mean that a time series of more than a day has to be measured to get a small number of CRPs (say, ten per group belonging to a fixed point).

Fortunately, the solution to this problem is quite simple. Instead of fitting just one linear relation that predicts one complete cycle ahead, many of these linear predictions were fitted to trajectories belonging to the CRPs, each only predicting a nearby map ahead. The sampling frequency was set to 32 samples per driving cycle and for a number of $N=32$ sections, the following linear model was fitted to the data:

$$\begin{bmatrix} \theta^{n+1} \\ \theta^{n} \\ 1 \end{bmatrix} = \mathbf{M}^n \begin{bmatrix} \theta^{n} \\ \theta^{n-1} \\ 1 \end{bmatrix}, \quad \mathbf{M}^n \begin{bmatrix} m_{11}^n & m_{12}^n & m_{23}^n \\ 1 & 0 & 0 \\ 0 & 0 & 1 \end{bmatrix}, \tag{11}$$

and $n=0,1,2,\ldots,31$. Note that the choice of the number of $N=32$ sections is not so important; another number of the same order of magnitude would give the same results. Obviously, the angles on map 0 should be identical to those on map N,

$$\begin{bmatrix} \theta^{N} \\ \theta^{N-1} \\ 1 \end{bmatrix} = \mathbf{M}^{N-1}\mathbf{M}^{N-2}\cdots\mathbf{M}^{0} \begin{bmatrix} \theta^{0} \\ \theta^{-1} \\ 1 \end{bmatrix}. \tag{12}$$

By setting $\theta^N=\theta^0$ and $\theta^{N-1}=\theta^{-1}$, the fixed point on map 0 will be obtained, from which all other fixed points can be computed. Comparison with Eq. (10) would suggest that application of Eq. (12) is no improvement, since it has the same form. But the one-step-ahead Jacobians can now be fitted to trajectories that do not follow the periodic orbit close for a complete cycle. So these may now also contain information of the unstable directions. Another improvement is that the obtained description of the UPO is smooth, meaning that from section to section the description agrees with the experimental (fitted) data. This means that although there could be an error between the estimate of the UPO and the real UPO, it is very close to trajectories that can actually occur in the system, so no large control actions are expected to be required. Figure 7 shows two UPOs (a) and (b), calculated as described above. UPO (a) corresponds with one complete rotation per driving period and UPO (b) with three rotations in the other direction.

A periodic orbit could be determined more accurately if the models could adequately predict further into future. A linear model like the one described above will only be valid for a long term prediction when it is restricted to a very small region around the fixed points. In that situation, the probability of finding CRPs becomes very small for this pendulum, and in general for higher dimensional systems this will even be worse. So one could think of using a nonlinear prediction model, like a neural net, which is valid in a larger region around the fixed point with the advantage that (much) more data can be included in case of the same time series. This will be at the cost of more model parameters that are necessary, but it could still be advantageous because the number of CRPs found increases quickly with the maximum allowed distance between the pairs; see Fig. 8.

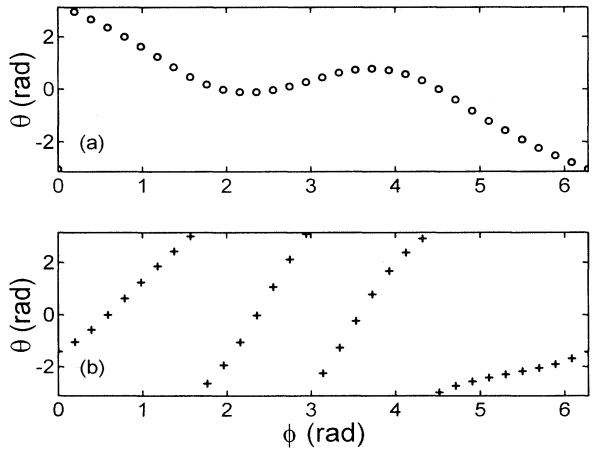

FIG. 7. Two UPOs that were stabilized. In both graphs 32 (fixed) points are plotted. UPO (a) corresponds to one rotation per driving cycle, while UPO (b) corresponds to three rotations in the other direction.

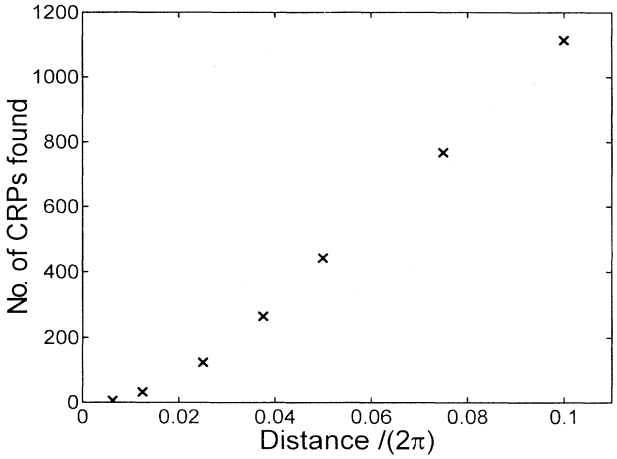

FIG. 8. Number of CRPs found from a time series of 45 000 cycles, as a function of the distance between two successive points. For a distance $|\vec{Z}^{n+1}-\vec{Z}^{n}|<0.025\times 2\pi$, only 33 CRPs are found to belong to several fixed points. So per fixed point, only a very small number of CRPs remains. Increasing the distance results in much more CRPs, but also in nonlinearity.

V. FIT OF THE PREDICTING LINEAR MODELS

Once the periodic orbit has been extracted from time series as it is described above, the number of control sections and the delay time T_D must be chosen to fit the predicting linear models of Eq. (4). The choice was made to measure the Jacobians $\mathbf{A}^n$ from the unperturbed system using the same time series from which the periodic orbits were estimated. In principle, one would like to use a large number of control sections to get an almost continuous control. However, if the time between two control sections is short, a perturbation that is applied for estimating the effect of the control parameter $\vec{B}$ will hardly get time to influence the system enough to be measurable. Therefore $\vec{B}$ cannot be estimated from Eq. (4) directly. A number of eight sections appeared to be sufficiently small to obtain a measurable effect of the control parameter. The delay time T_D was taken as 25% of the time between two sections. It could be up to nearly 100% of this time without another control parameter term (δp^{n-2}) being

required. If this time would go to nearly zero, it would correspond to measuring the angular velocity, however, with a large experimental error due to sampling. The largest estimated error of the Jacobian $\mathbf{A}^n$ was about five times the accuracy of the angle reading; it meant that the linearization was not really adequate, but sufficient for control purposes.

The next step was to estimate all $\vec{B}_0^n$ and $\vec{B}_1^n$ from a time series with a perturbed control parameter. A time series with a constant perturbation ($\delta p^n = C$, all n) could not be used because in that case $\delta p^n = \delta p^{n-1} = C$, so $\vec{B}_0^n$ and $\vec{B}_1^n$ cannot be distinguished from each other. Therefore, the time series had to be measured with a changing control parameter. A simple choice was made to switch *on* the control parameter for even control sections ($\delta p^{\text{even}} = C$) and *off* for odd sections ($\delta p^{\text{odd}} = 0$). All control sections of this time series were searched for points close to the fixed point of the selected UPO. In order to get points in a linear region, only points with a very small distance (less than 0.02π rad) from the fixed points were selected. A time series with 45 000 points resulted in about 10 to 20 points per UPO for each section. Using the estimated Jacobians $\mathbf{A}^n$, the elements of $\vec{B}_0^{\text{even}}$ and $\vec{B}_1^{\text{odd}}$ were estimated from Eq. (4). The other half of all vectors $\vec{B}$ ($\vec{B}_0^{\text{even}}$ and $\vec{B}_1^{\text{odd}}$) were calculated in the same way from another time series recorded with $\delta p^{\text{even}} = 0$ and $\delta p^{\text{odd}} = C$. The constant perturbation C was 10% of the amplitude of the torque applied. Lower values resulted in an effect of the control parameter that was too small (and a large error in $\vec{B}$), and at larger values the system did not come sufficiently close to the periodic orbit anymore. As expected, the effect of the previous control action ($\vec{B}_1$) was smaller than that of the present control action ($\vec{B}_0$), typically 60% smaller.

In this way, the effect of the control parameter of the UPO of Fig. 7(a) was determined. After a short transient time in which the system needed to come close to a fixed point, the control algorithm could stabilize this UPO. Figure 9 shows an example of this, while Fig. 10 shows a typical, corresponding control signal superimposed on the permanent sinusoid torque. It was found that the control became less sensitive to sudden large external perturbations (viz., moving the pendulum apparatus) if the control parameter was given its maximal allowable value $\delta p^{\max}$ when stabilization was almost lost. For example, if the maximal allowable value of δp was chosen between -10 and 10% of the amplitude of the driving torque, then if the control algorithm Eq. (8) would calculate a control parameter $\delta p = -15\%$, it would be set to $\delta p = -10\%$.

For the UPO of Fig. 7(b) the approach described above failed because the perturbed system never came sufficiently close to some of the fixed points of the UPO. This was probably due to a change in position of the attractor in state space caused by the perturbations. To overcome this problem, the effect of the control parameter was measured in another way. The system was not perturbed until it came close to a fixed point. Then the control parameter was given a *constant* value between two control sections (10% of the driving amplitude). Once there were enough (say 20) measurements collected around a fixed point on one of the sections, no further perturbations were made when the system came close to it. This was done because these perturbations could cause the system's trajectory to leave the region near the UPO, before the fixed point on the next section could be approached. In this way, enough data was obtained to calculate the effect of the control parameter, and the UPO was stabilized as well. The major difference with perturbing the system every control section to measure the effect of the control parameter, is that in this way, locations of fixed points have to be determined first. This means that for every UPO to stabilize, a new time series for that UPO should be measured.

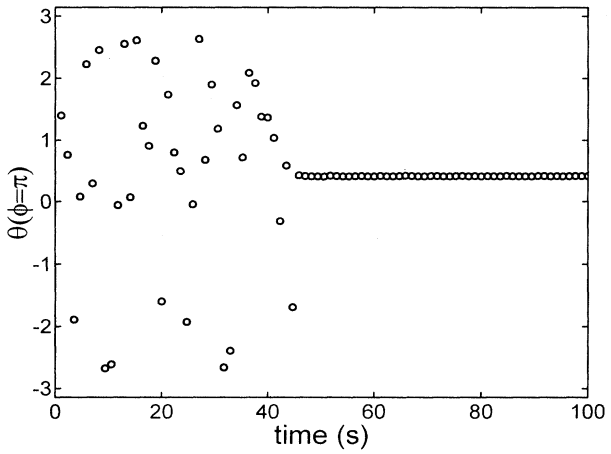

FIG. 9. After starting an experiment, it takes more than 40 sec before the system comes close to a fixed point after which UPO (a) can be stabilized.

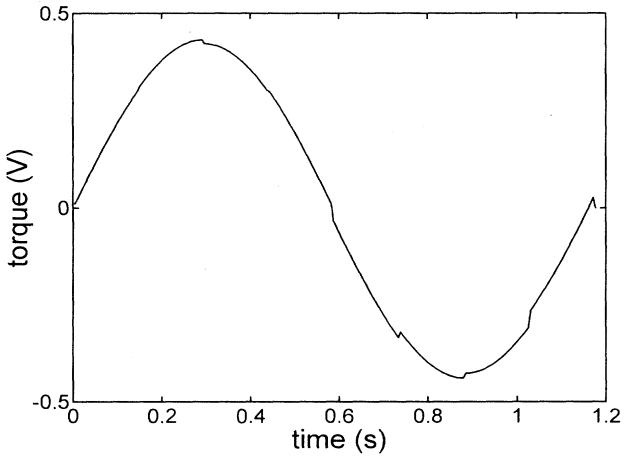

FIG. 10. Typical example of the continuously applied sinusoid torque with a control signal superimposed on it. Note that the use of $N = 8$ surfaces of section for control, corresponds to the eight jumps in the sine of this graph.

VI. SYSTEMATIC DEVIATION FROM UPO

Stabilization of the periodic orbit of Fig. 7(b) showed a remarkable result. One would expect that once the system comes close to a fixed point, the control algorithm needs a short transient time in which the UPO becomes stabilized. After this time, the trajectory should be almost exactly on the periodic orbit and the control actions needed should be almost zero, only due to some small errors in the pendulum's angle reading (noise) and the linearization of the models. However, as Fig. 11 shows, the control value for some control sections did not have a zero mean, but a systematic nonzero control value. In general this is an undesired phenomenon, because an attractive property of controlling a chaotic system is that only small, i.e., low energy demanding, control actions should be adequate. It was originally thought that the systematic offset of the control parameter was caused by the nonlinearity of the pendulum. As a result there was a bad fit of the linear models, so there were significant errors in the fixed points estimates. When controlling the UPO the control algorithm would try to steer the system towards locations in state space that were not the fixed points. This would require a nonzero mean control parameter to stabilize the approximate periodic orbit. Although later on it was found that there was an *experimental* reason for the error in the estimated fixed points, at that time it was thought that the nonlinearity was the cause. It was tried to fit the linear models to data closer to the UPO than before, using a time series obtained from the *controlled* UPO. All data of this time series was located near the UPO, in contrast to a time series of the *uncontrolled* pendulum where data of this quality only occurs one or two times an hour. A relation similar to Eq. (4) was fitted directly to data of the *controlled* pendulum, but now an intercept was also taken into account, as it appeared to be an essential term for a proper prediction:

$$\delta\vec{Z}^{n+1}=\mathbf{A}^n\delta\vec{Z}^n+\vec{C}^n+\vec{B}_0\delta p^n+\vec{B}_1\delta p^{n-1}\ . \tag{13}$$

Now a new estimate of the fixed points was obtained, calculated similar as before by using that the control section at time $n=0$ is identical to that at time $n=N=8$,

$$\begin{bmatrix}\delta\theta(t^n)\\ \delta\theta(t^n-T_D)\\ 1\end{bmatrix}_{*,n=N}=P\begin{bmatrix}\delta\theta(t^n)\\ \delta\theta(t^n-T_D)\\ 1\end{bmatrix}_{*,n=0}, \tag{14}$$

with

$$\mathbf{P}=\begin{bmatrix}\mathbf{A}^{N-1} & & \vec{C}^{N-1}\\ 0 & 0 & 1\end{bmatrix}\times\begin{bmatrix}\mathbf{A}^{N-2} & & \vec{C}^{N-2}\\ 0 & 0 & 1\end{bmatrix}\cdots\begin{bmatrix}\mathbf{A}^{0} & & \vec{C}^{0}\\ 0 & 0 & 1\end{bmatrix}. \tag{15}$$

The calculation of what was thought to be a better description of the fixed points, showed that all fixed points were shifted nearly 2°. This is a result of the initialization of the angle at $\theta\equiv 0$, at the start of an experiment when the pendulum is at rest. The pendulum device has only a small base and stands on a soft, shock absorbing layer, so it is possible that the metal base is not always in the same horizontal position. After the pendulum device was brought to a fixed position, the control parameter obtained a zero mean again during control. So the assumption that the linear models had a large error because of severe nonlinearity was not correct.

However, although for the pendulum the problem of the shifted UPO was very easy to solve by fixing the position of the apparatus, the approach described above could also be used for the control of chaotic systems that are not completely stationary. If the position of the UPO in state space changes slowly compared to the time scale of the controlled orbit (drift), this will be reflected in the controlled behavior. From this, linear models can be fitted and a shift in position can be calculated so that the control algorithm can still stabilize the same UPO, but now on its changed position, so that still only small control actions are needed. On doing this, one should keep in mind that the data obtained from a controlled UPO is not spread uniformly around the UPO in state space, but only in a narrow region near the UPO. See, for example, Fig. 11(b), where no points are located in the controlled system for negative values of δp. To avoid the dangers of extrapolation, one could add some noise to the control parameter such that the UPO is still stabilized, but the trajectory moves in a wider region around it, so that the linear models will be valid in a wider region.

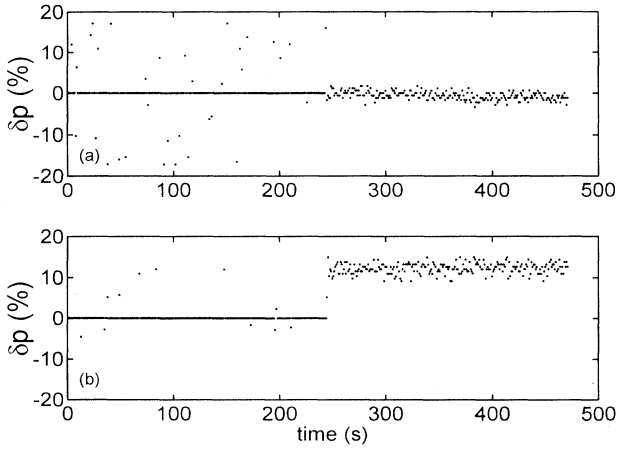

FIG. 11. Applied control signal δp in percentage of amplitude of sinusoid torque, for stabilizing UPO (b). (a) when the UPO becomes stabilized after 250 sec the control parameter has zero mean for one section, but another section (b) shows a systematic offset.

VII. CONCLUDING REMARKS

Periodic orbits of the chaotic pendulum can be stabilized by using a semicontinuous control (SCC) method. In contrast to control based on one section, such as the original OGY method, it does not fail for the pendulum with its large unstable eigenvalue (around ten). The sys-

tem state can be represented by delay coordinates with the advantage that only one system variable has to be measured. Although the use of delay coordinates causes that a previous control parameter δp^{n-1} must be taken into account, this turns out to be no problem for actually controlling the pendulum.

The UPOs of the pendulum could be estimated by fitting local linear models (Jacobians) with the advantage that (i) information from unstable directions is used and (ii) less data is needed compared to fitting a linear predictor one complete cycle ahead. It is important that this position of an UPO is estimated accurately because a deviation from the true UPO can result in systematic nonzero mean control actions. In case of an application, this is undesired in general, because the smaller the control actions, the easier they are to make.

Measuring the effect of the control parameter, viz., estimating $\vec{B}_0^n$ and $\vec{B}_1^n$, is more difficult than fitting the Jacobians. Taking a simple time series with the control parameter being switched on and off when two control sections are crossed, *may* lead to estimates of $\vec{B}_0^n$ and $\vec{B}_1^n$, for $n=1,\ldots,N$, good enough to stabilize the UPO. However, this frequent applying of a control action to measure its effect, may be the reason that the system does not come close to some UPO's fixed points anymore. In that case, $\vec{B}_0^n$ and $\vec{B}_1^n$ cannot be fitted to trajectories close to the UPO. In that case one could try to perturb the system more randomly, hoping that all positions of the unperturbed attractor are still visited. We used a different approach that successfully gave the effect of the control parameter: perturbing the system only when it comes close to a fixed point.

Once a periodic orbit has been stabilized, the measured time series contains useful information of the system's behavior near the UPO. This is in contrast to the uncontrolled system that visits the region around an UPO at a much lower frequency. This information can be used to recalculate the position of all fixed points, which can be advantageous when a system changes slowly in time (drift) or when the fixed points were calculated from a short time series with a high noise level. In both situations, the control will become more stable, and systematic nonzero mean control actions will reduce towards zero mean.

In a future work, we will try to extend a SCC method to higher dimensional systems. The final aim of the work is to experimentally control the chaotic hydrodynamics of the gas-solids fluidized bed reactor [11] to enhance chemical conversion and selectivity.

ACKNOWLEDGMENTS

The authors are grateful to Professor Dr. F. Takens for valuable comments upon the reading of the draft of this paper. The work is supported in part by the Research Stimulus Fund of Delft University of Technology, in part by the Netherlands Foundation for Chemical Research (SON) with financial aid from the Netherlands Technology Foundation (STW), and in part by Setpoint Ipcos and Akzo Nobel. All this support is gratefully acknowledged.

[1] E. Ott, C. Grebogi, and J. A. Yorke, Phys. Rev. Lett. **64**, 1196 (1990).
[2] T. Shinbrot, C. Grebogi, E. Ott, and J. A. Yorke, Nature **363**, 411 (1993).
[3] J. Starret and R. Tagg, Phys. Rev. Lett. **74**, 1974 (1995).
[4] K. Pyragas, Phys. Lett. A **170**, 421 (1992).
[5] A. Kittel, J. Parisi, and K. Pyragas, Phys. Rev. Lett. A **198**, 433 (1995).
[6] S. Bielawski, M. Bouazaoui, D. Derozier, and P. Glorieux, Phys. Rev. A **47**, 3276 (1993).
[7] B. Hübinger *et al.*, Phys. Rev. E **5**, 932 (1994).
[8] C. Reyl, L. Flepp, R. Badii, and E. Brunn, Phys. Rev. E **47**, 267 (1993).
[9] U. Dressler and G. Nitsche, Phys. Rev. Lett. **68**, 1 (1992).
[10] B. Hübinger, R. Doerner, and W. Martienssen, Z. Phys. B **90**, 103 (1993).
[11] C. M. van den Bleek and J. C. Schouten, Chem. Eng. J. (Lausanne) **53**, 75 (1993).